Electronic structure and ionicity of actinide oxides from first principles

L. Petit,[1,2,*] A. Svane,[1] Z. Szotek,[2] W. M. Temmerman,[2] and G. M. Stocks[3]
[1]*Department of Physics and Astronomy, Aarhus University, DK-8000 Aarhus C, Denmark*
[2]*Daresbury Laboratory, Daresbury, Warrington WA4 4AD, United Kingdom*
[3]*Materials Science and Technology Division, and Center for Defect Physics, Oak Ridge National Laboratory, Oak Ridge, Tennessee 37831, USA*

(Received 10 July 2009; revised manuscript received 26 November 2009; published 7 January 2010)

The ground-state electronic structures of the actinide oxides AO, A_2O_3, and AO_2 (A=U, Np, Pu, Am, Cm, Bk, and Cf) are determined from first-principles calculations, using the self-interaction corrected local spin-density approximation. Emphasis is put on the degree of f-electron localization, which for AO_2 and A_2O_3 is found to follow the stoichiometry, namely, corresponding to A^{4+} ions in the dioxide and A^{3+} ions in the sesquioxides. In contrast, the A^{2+} ionic configuration is not favorable in the monoxides, which therefore become metallic. The energetics of the oxidation and reduction in the actinide dioxides is discussed, and it is found that the dioxide is the most stable oxide for the actinides from Np onward. Our study reveals a strong link between preferred oxidation number and degree of localization which is confirmed by comparing to the ground-state configurations of the corresponding lanthanide oxides. The ionic nature of the actinide oxides emerges from the fact that only those compounds will form where the calculated ground-state valency agrees with the nominal valency expected from a simple charge counting.

DOI: 10.1103/PhysRevB.81.045108 PACS number(s): 71.27.+a, 71.15.Mb, 71.20.−b, 71.30.+h

I. INTRODUCTION

Actinide oxides play a dominant role in the nuclear fuel cycle.[1] For many years, uranium dioxide has been the main fuel component in commercial nuclear reactors. The "burning" of UO_2 results in considerable amounts of Np and Pu isotopes, as well as smaller quantities of minor actinides such as Am, Cm, Bk, and Cf. In original, "once through" reactors, the highly radioactive waste that was produced resulted in very troublesome long-time storage requirements; particularly of Pu. However, it was soon realized that the Pu could be reprocessed from the spent fuel and used as alternative fuel in a new generation of reactors. The environmental and energy production issues apart, the fact that Pu is obtained from the decommisioning of nuclear weapons is yet another important consideration concerning its use as nuclear fuel. A mixture of UO_2 and PuO_2, where Pu is blended with either natural or depleted uranium, constitutes the preferred, Pu containing, fuel in existing nuclear reactors. Lately, Np, as well as the minor actinides that accumulate during nuclear reactor operation, are also being considered for reprocessing.[2] Once separated from the spent fuel, these actinides can either be incorporated in durable ceramic waste for safe long-time storage (and possible later recovery) or transmuted from long-lived isotopes to less radiotoxic short-lived isotopes through irradiation, thus taking part in the fuel cycle and reducing the long-term nuclear-waste management problem. Again oxides are being considered both with respect to the materials being used as fission/transmutation targets (AO_2) (Ref. 3) and for the direct storage in the shape of durable ceramic glasses (AO_2,A_2O_3).[2] For example, PuO_2 has long been the compound of choice for depositing Pu in long-time repositories, given the observed stability with respect to oxidation.[4]

Regarding their behavior under both reactor operation and storage conditions, it is crucial to understand the thermochemistry, thermophysics, and materials science of the actinide compounds. Given the toxicity of the materials involved, computer simulations, such as thermodynamic modeling[5] or, as in the present paper, electronic-structure calculations can provide fundamental insights at a level not achievable through experiment alone. Here we wish to focus specifically on the f electrons, their contribution to the ground-state electronic properties of the actinide oxides, the role they play with regards to stability toward oxidation, and their behavior under ionic bonding conditions.

When modeling the electronic structure of actinide materials, the most distinguishing feature is the increasing importance of correlations across the series from U to Cf, as the nature of the f electrons changes from delocalized in the early actinides to localized in the later actinides.[6–8] Electronic-structure calculations, based on the local spin-density approximation (LSDA) to density-functional theory (DFT), do not take into account strong on-site correlations beyond the homogeneous electron gas, and therefore cannot adequately describe the localized phase of actinide materials. Thus the LSDA (Ref. 9) or even the generalized gradient approximation (GGA) (Ref. 10) (which extends beyond the LSDA by taking into account charge-density gradients), wrongly predicts a metallic ground state for UO_2, PuO_2, and Pu_2O_3, although the equilibrium lattice parameters and cohesive properties are found to be in rather good agreement with experiment.[10–12]

A number of schemes have been developed that augment the standard band-structure framework to include the effects of strong correlations on the electronic structure. In the LDA+U approach[13,14] an effective Coulomb parameter U is introduced that separates the f manifold into the upper and lower Hubbard bands and removes f degrees of freedom from the Fermi level. The more advanced dynamical mean-field theory (DMFT) approach provides a description of the competing trends toward localization on the one hand and itineracy on the other hand by taking into account the local

quantum fluctuations missing in the static LDA+U treatment;[15,16] albeit still at the cost of the introduction of the U parameter. The hybrid density-functional[17] theory implements an exchange-correlation functional where a fraction of the exact nonlocal exchange interaction from Hartree-Fock theory is mixed with the local or semilocal exchange energy of LSDA or GGA with the result that the troublesome effects of the known self-interaction error present in the standard LSDA and GGA calculations are reduced.

The self-interaction corrected (SIC)-LSD approach[18] used in the current work removes the self-interaction error that occurs in the LSDA, thereby leading to an improved description of the static Coulomb correlations of the f electrons. The self-interaction correction associates an energy gain with electron localization, which competes with the opposing trend of band formation, providing a dual picture of combined localized and bandlike f electrons. The method is fully *ab initio* as both kinds of electrons are treated on an equal footing, with no adjustable parameters. A comparative study of MnO, involving SIC-LSD, LDA+U, and the hybrid functional methods, was published by Kasinathan *et al.*[19]

The present paper is organized as follows. In the following section, we give a short introduction to the SIC-LSD band-structure method. In Sec. III, we present our SIC-LSD results for the ground-state properties of (A) the monoxides, (B) the sesquioxides, and (C) the dioxides where we also consider oxidation/reduction energies. In Sec. IV, we give a summarizing discussion of the results, also concerning the relation between f-electron localization and oxidation by comparing to the lanthanide oxides. The conclusion of our paper is presented in Sec. V.

II. SIC-LSD METHODOLOGY

The LSD approximation to the exchange and correlation energy introduces an unphysical interaction of an electron with itself[18] which, although insignificant for extended band states, may lead to uncontrollable errors in the description of atomiclike localized states, for example, the f electrons in the later actinides. The SIC-LSD method[20,21] corrects for this spurious self-interaction by adding to the LSD total-energy functional an explicit energy contribution for an electron to localize. The resulting, orbital-dependent, SIC-LSD total-energy functional has the form

$$E^{\text{SIC-LSD}} = E^{\text{LSD}} + E_{so} - \Delta E_{sic}, \tag{1}$$

where

$$E^{\text{LSD}} = \sum_{\alpha}^{occ.} \langle \psi_\alpha | -\nabla^2 | \psi_\alpha \rangle + U[n] + V_{ext}[n] + E_{xc}^{\text{LSD}}[n_\uparrow, n_\downarrow], \tag{2}$$

$$E_{so} = \sum_{\alpha}^{occ.} \langle \psi_\alpha | \xi(\vec{r}) \vec{l} \cdot \vec{s} | \psi_\alpha \rangle, \tag{3}$$

$$\Delta E_{sic} = \sum_{\alpha}^{occ.} \delta_\alpha^{\text{SIC}} = \sum_{\alpha}^{occ.} \{U[n_\alpha] + E_{xc}^{\text{LSD}}[n_\alpha]\}. \tag{4}$$

Here the sums run over all occupied electron states ψ_α. As usual, the LSD total-energy functional [Eq. (2)] is decomposed into the kinetic energy, the Hartree energy, the interaction energy with the atomic ions, and the exchange and correlation energy. The spin-orbit interaction [Eq. (3)] couples the band Hamiltonian for the spin-up and spin-down channels, i.e., a double secular problem must be solved. The spin-orbit parameter,

$$\xi(r) = -\frac{2}{c^2}\frac{dV}{dr}$$

in atomic Rydberg units, is calculated from the self-consistent potential. The self-interaction energy [Eq. (4)] consists of the self-Coulomb and self-exchange-correlation energies of the occupied orbitals ψ_α with the orbital charge density n_α.

With regards to determining the ground-state electronic structure of a given actinide compound, the advantage of the SIC-LSD total-energy functional in Eq. (1) is that different valency scenarios can be explored by assuming atomic configurations with different total number of localized f configurations. For itinerant states, the self-interaction $\delta_\alpha^{\text{SIC}}$ vanishes identically while for localized (atomiclike) states $\delta_\alpha^{\text{SIC}}$ may be appreciable. Thus, the self-interaction correction constitutes a negative-energy contribution gained by an electron upon localization, which competes with the band-formation energy gained by the electron if allowed to delocalize and hybridize with the available conduction states. Different localized/delocalized configurations are realized by assuming different numbers of localized states—here f states on actinide-atom sites, and the investigated configurations range from the LSD scenario, where the electrons, including all the f electrons, are treated as itinerant electron states to the fully localized scenario, where all the f electrons are treated as localized. For s and p states, $\delta_\alpha^{\text{SIC}}$ is never competitive compared to the corresponding gain in band-formation energy and turns out to be positive.

Since the different localization scenarios constitute distinct local minima of the same energy functional, $E^{\text{SIC-LSD}}$, their total energies may be compared and the global energy minimum then defines the ground-state total energy *and* the valence configuration of the actinide ion. This latter is defined as the integer number of electrons available for band formation,

$$N_{val} = Z - N_{core} - N_{\text{SIC}}, \tag{5}$$

where Z is the atomic number, N_{core} is the number of atomic core electrons, and N_{SIC} is the number of SIC-localized f electrons. In the remainder of this paper we will be using two interchangeable nomenclatures, f^n and A^{m+}, to describe the configuration of the actinide ion, implying $n=N_{\text{SIC}}$ and $m=N_{val}$, respectively. The total number of f electrons may be larger than n, since, in addition to the n localized f states, the band states also contribute to the total f count on a given ion. Note that our calculated valencies refer to the number of

actinide electrons that contribute to bonding, and thus do not necessarily coincide with the nominal (ionic) valency of a compound. For PuO_2, for example, the Pu^{4+} would agree with an ionic picture while the Pu^{3+} and Pu^{5+} valency configurations would indicate more covalent behavior.

The SIC-LSD approach is fully *ab initio*, as both localized and delocalized states are expanded in the same set of basis functions and are, thus, treated on an equal footing. If no localized states are assumed, $E^{\text{SIC-LSD}}$ coincides with the conventional LSD functional, i.e., the Kohn-Sham minimum of the E^{LSD} functional is also a local minimum of $E^{\text{SIC-LSD}}$.

Given the total-energy functional $E^{\text{SIC-LSD}}$, the computational procedure is as for the LSD case, i.e., minimization is accomplished by iteration until self-consistency. In the present work, the electron wave functions are expanded in the linear-muffin-tin-orbital (LMTO) basis functions.[22] The atomic spheres approximation (ASA) is used, whereby the crystal volume is divided into slightly overlapping atom-centered spheres of a total volume equal to the actual volume. A known shortcoming of the ASA is that different crystal structures have different degrees of overlap of the ASA spheres resulting in substantial *relative* errors in the evaluation of the total energy. While this inhibits the comparison of energies of different crystal structures, when comparing the energies of different localization scenarios within the same crystal structure the ASA error is of minor influence. To improve the packing of the structure empty spheres have been introduced on high-symmetry interstitial sites. Two uncoupled energy panels have been considered when constructing the LMTOs to ensure an accurate description of semicore states. Determining the lowest-energy solution of the orbital functional [Eq. (1)] requires careful and thorough minimimization with respect to both the number and symmetries of the localized orbitals.[12,23] The LS-coupling scheme is adopted for the localized f states by starting the iterations with Wannier states of appropriate symmetry. During iteration to self-consistency the symmetry of the Wannier states may change, however grossly retaining their overall characteristics due to the fact that the energy scale of spin-orbit interaction is smaller than that of exchange but larger than that of crystal field for the f states.

III. RESULTS

A. Actinide monoxides

1. Background information

There exists to date no convincing evidence that actinide oxides can form in the 1:1 stoichiometry. The experimental lattice parameters that we cite in Table I come from early reports on these compounds, and have so far not been confirmed. There have been no claims of bulk UO having ever been synthesized, and reports of an UO surface phase on U metal for low exposures to O,[24,25] and UO thin films[26] could not be reproduced.[27] It has been suggested that the observed thin films actually represent uranium oxynitrides (UN_xO_{1-x}) and oxycarbides (UC_xO_{1-x}), which form in the presence of N_2 or C, and at low oxygen pressure.[28] It has similarly been concluded that neither bulk NpO nor a corresponding NpO surface phase will form.[29,30] Preparation of PuO and AmO,[31] as well as possibly BkO,[32] has been neither substantiated nor has it been dismissed.

TABLE I. Actinide monoxide data. Column 2: ground-state configuration. Column 3: energy difference in eV between the ground state and the ideal ionic divalent configuration. Column 4: ground-state density of states at the Fermi level (in units of states per eV and formula unit). Column 5: calculated lattice parameters a_0^{calc} (in Å). Column 6: experimental lattice parameter a_0^{exp} (in Å), where known (measurements on UO, and NpO refer to thin-film data, measurements on PuO, AmO, and BkO refer to bulk data).

AO	Config.	$E_{GS}-E_{II}$	$n(E_F)$	a_0^{calc}	a_0^{exp}
UO	f^1 (U^{5+})	−1.93	5.8	4.94	4.92[a]
NpO	f^3 (Np^{4+})	−1.73	1.1	4.99	5.01[b]
PuO	f^5 (Pu^{3+})	−0.58	5.9	5.13	4.960[c]
AmO	f^6 (Am^{3+})	−0.14	7.3	5.14	5.045[c]
CmO	f^7 (Cm^{3+})	−1.14	2.6	5.01	
BkO	f^8 (Bk^{3+})	−0.65	1.4	4.97	4.964[d]
CfO	f^9 (Cf^{3+})	−0.20	9.5	4.97	
EsO	f^{10} (Es^{3+})	0.00	4.0	4.92	
EsO	f^{11} (Es^{2+})	0.00	0.0	5.06	

[a]Reference 26.
[b]Reference 33.
[c]Reference 31.
[d]Reference 32.

2. SIC-LSD electronic structure

We have calculated the electronic structure of the monoxides with the SIC-LSD method in order to establish the ground-state properties for the hypothetical NaCl structure. Ferromagnetic arrangement of the spins has been assumed in these calculations. The results are summarized in Table I. We find the trivalent configuration to be energetically most favorable for all the monoxides, except UO and NpO that, respectively, prefer the U^{5+} (f^1) and Np^{4+} (f^3) ground-state configurations. Concerning UO, it should be noted here that

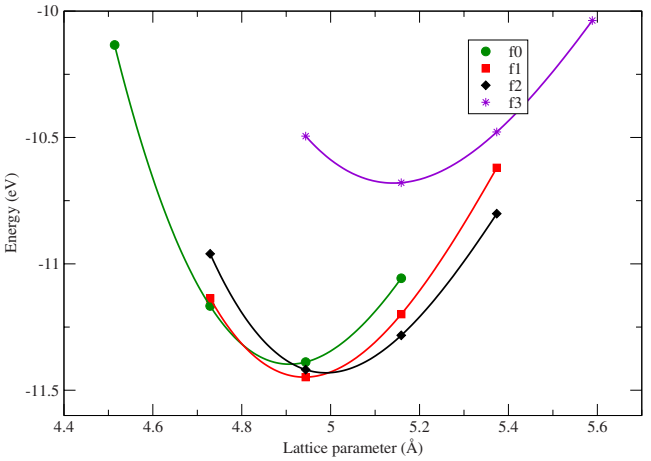

FIG. 1. (Color online) Total energy of UO in the rock-salt structure assuming different localized/delocalized f-electron scenarios.

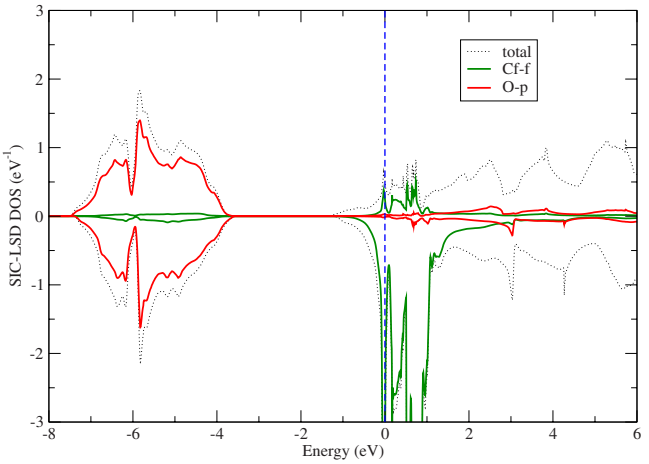

FIG. 2. (Color online) Density of states for CfO in the ground-state configuration with nine f electrons localized on the Cf^{3+} ion. The majority (minority) spin components are displayed as positive (negative) values. The energy is measured in eV relative to the Fermi level, which falls amidst the minority Cf f bands. The localized Cf f states are not shown, as they occur well below the valence band.

even though we find the Uf^1 configuration to be the ground state, this energy scenario is close to degenerate with the fully itinerant LSD (f^0) and f^2 scenarios, as shown in Fig. 1. This indicates that the f-electron manifold lingers between the localized and delocalized pictures, i.e., correlations are strong but not to the degree for full localization to occur. This agrees with earlier results by Brooks *et al.*,[34] where the electronic structure of UO was calculated assuming itinerant f electrons, and which resulted in a calculated lattice parameter of 4.88 Å, i.e., only slightly overbinding with respect to the "experimental" value of 4.92 Å. The SIC-LSD calculated lattice parameters of the f^1 and f^2 configurations, respectively, 4.94 and 4.99 Å, indicate a slight overlocalization. Overall, the calculated lattice parameters are in rather good agreement with the early experimental values. However, as there is no convincing subsequent experimental evidence in support of the fact that monoxides really exist in nature, one should not put too much weight on the agreement between theory and experiment.

For the monoxides beyond UO, the LSD configuration never becomes even remotely energetically favorable. For NpO a tetravalent ground state [$Np^{4+} \equiv Np(f^3)$] is found whereas a trivalent ground-state configuration is established for the remaining monoxides. In their respective ground states, the monoxides are metallic, as can be seen from the nonzero density of states (DOS) at the Fermi energy (column 4 of Table I). As a representative example, the DOS of CfO is depicted in Fig. 2. The O atom has two unoccupied p states, and in the corresponding monoxide, the p band can accommodate two electrons from the actinide atom through charge transfer and hybridization while the remaining valence electrons, including the delocalized f electrons, start filling the conduction band, with the Fermi level pinned to the narrow f band. The localized f states are not shown in Fig. 2, as they lie well below the valence band. The ionic insulating picture would be realized if additional f states preferred to localize, giving rise to the divalent configuration. In Table I (column 3) the calculated energy differences, $E_{GS} - E_{II}$, between the ground-state configuration and the divalent configuration are shown. It is clear that the nominal ionic $A^{2+}O^{2-}$ scenario does not become energetically favorable for any of the monoxides. Nevertheless this energy difference is seen to decrease from UO to AmO, and again from CmO to CfO, which is in agreement with the trends toward increasing localization due to the actinide contraction. At AmO the trivalent configuration is thus only marginally more favorable than the divalent half-filled shell configuration. For EsO, the energy difference between the trivalent and divalent scenarios vanishes, indicating degeneracy between these two configurations. In Table I, both "ground-state" scenarios are therefore quoted, with $E_{GS} - E_{II}$ equal to zero. The overall picture of nonionic ground states in the monoxides, that emerges from our SIC-LSD calculations, confirms the results from early molecular cluster calculations on the heavy actinide monoxides by Gubanov *et al.*,[35] where considerable covalency due to mixing of O p and A f orbitals was found.

B. Actinide sesquioxides

1. Background information

Bulk phases of U_2O_3 as well as Np_2O_3 do not exist in nature, and have never been synthesized but thin films of Np_2O_3 have been found to form on the surface of Np metal.[30] From Pu onward, the sesquioxides are stable and have been synthesized. Beyond Pu, the sesquioxides crystallize in three different crystal structures, respectively, the hexagonal La_2O_3 structure (A form), the cubic Mn_2O_3 structure (C form), and the monoclinic Sm_2O_3 structure (B form). Pu_2O_3 has been synthesized only in the A and C forms. The X-ray photoelectron spectroscopy (XPS) measurements on sesquioxides from Pu_2O_3 to Cf_2O_3 have been reported,[36–38] and the absence of features at the Fermi level points toward the localized nature of the 5f electrons in these compounds. This indicates that they are semiconductors or insulators, in agreement with the ideal nominal picture of $A_2^{3+}O_3^{2-}$, although no values for the energy gaps can be found in the literature.

There exist relatively few calculations of the electronic structure of the actinide sesquioxides. Prodan *et al.*[39] have studied Pu_2O_3 (A form) with the help of hybrid density-functional theory, comparing a number of functionals. They have found that unlike in the LSD and GGA approximations, using the Heyd-Scuseria-Ernzerhof (HSE) screened Coulomb functional leads to an insulating antiferromagnetic solution, in good agreement with experiment, with the calculated gap value of 2.78 eV [3.50 eV for the Perdew-Burke-Ernzerhof (PBE0) hybrid functional]. The antiferromagnetic insulating nature of Pu_2O_3 has similarly been retrieved from electronic-structure calculations by respectively Jomard *et al.*[12] and Sun *et al.*,[40] based on the (LDA/GGA)+U approximation. The magnitudes of their band gaps are found to depend strongly on the value chosen for the on-site Coulomb interaction U. For $U=4$ eV, and depending on the details of the functional, energy gaps ranging from 1 to 2 eV were obtained.

TABLE II. Actinide sesquioxide data: Column 2: ground-state configuration of actinide ion. Column 3: calculated energy gap, E_{gap}, (in eV). Columns 4 and 5: calculated, V_{calc}, and experimental (Ref. 33), V_{exp}, equilibrium volumes in units of Å^3 per formula unit.

Compound	Ground state	E_{gap}	V_{calc}	V_{exp}
	C-type sesquioxides			
U_2O_3	f^2 (U^{4+})	0.00	83.17	
Np_2O_3	f^3 (Np^{4+})	0.00	84.40	
Pu_2O_3	f^5 (Pu^{3+})	0.75	89.42	82.73
Am_2O_3	f^6 (Am^{3+})	0.44	88.54	83.64
Cm_2O_3	f^7 (Cm^{3+})	0.32	86.98	83.10
Bk_2O_3	f^8 (Bk^{3+})	0.38	83.41	80.63
Cf_2O_3	f^9 (Cf^{3+})	0.47	82.60	79.59
	A-type sesquioxides			
Pu_2O_3	f^5 (Pu^{3+})	2.43	74.06	75.49
Am_2O_3	f^6 (Am^{3+})	2.54	73.34	74.73
Cm_2O_3	f^7 (Cm^{3+})	3.07	72.40	74.53
Bk_2O_3	f^8 (Bk^{3+})	2.73	70.10	72.71
Cf_2O_3	f^9 (Cf^{3+})	1.78	69.33	71.43

2. SIC-LSD electronic structure

In the present work the electronic structures of the sesquioxides from U_2O_3 to Cf_2O_3 has been calculated for both the cubic C form and the hexagonal A form. The results are summarized in Table II. The hexagonal A-type structure has space group $P\bar{3}m1$ (no. 164). The unit cell contains one formula unit with one oxygen at the origin, two oxygens at $\pm(1/3,2/3,z_O)$, and two actinide atoms at $\pm(1/3,2/3,z_A)$. While the c/a ratio has been measured for all the actindes from Pu to Cf, the internal parameters are only known for Pu (z_O=0.6451 and z_{Pu}=0.2408).[33] Hence we have performed our calculations for this structure with the experimental c/a ratios but using the internal parameters of Pu_2O_3 for all the other actinide sesquioxides.[41] The cubic C-type structure, also known as bixbyite, contains 40 atoms in the unit cell. In the SIC-LSD, the total-energy minimization procedure by the steepest-descent method, optimizing the orbitals on a large atom cluster, is considerably more time consuming than the standard LSD method for itinerant electron systems. We therefore approximate the bixbyite structure by the much simpler fluorite AO_2 structure, with 1/4 of the O atoms removed, namely, in the supercell consisting of four formula units the oxygen atoms at the origin and the cube center have been replaced by empty spheres. Using an ASA-based electronic-structure method we are not in a position to consider relaxations of the atomic coordinates for either the A-type or the C-type structure. The hope is, however, that the effect of such structural optimizations will be less important here since we only concentrate on relative energy differences corresponding to various localization/delocalization scenarios within a given structure. The primary goal is to discover trends that these energy differences lead to as a function of an actinide ion.

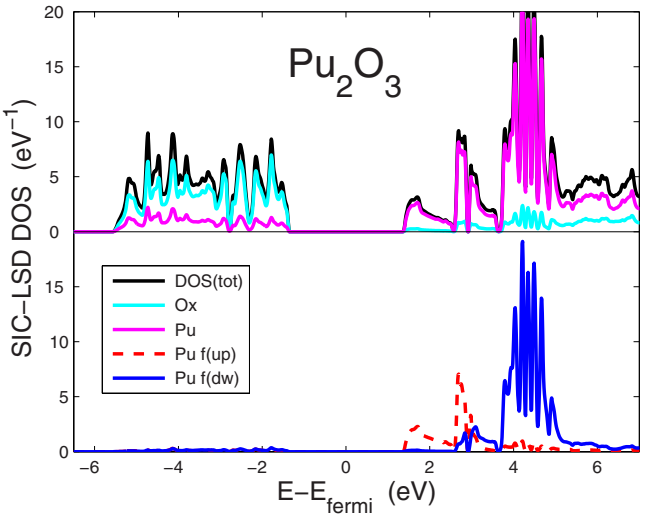

FIG. 3. (Color online) Density of states for A-type Pu_2O_3 in the trivalent ground-state configuration. The energy is in eV relative to the Fermi level, which is situated midgap. The DOS is in units of eV^{-1}/f.u. Upper panel: total black, Pu (violet/dark grey), and O (light blue/light grey) DOSs. Lower panel: the corresponding Pu f majority (dashed red) and minority (full blue) spin decomposed DOSs. Only the itinerant f states are shown.

The trivalent actinide configuration is found to be energetically favorable for all the compounds, apart from U_2O_3 and Np_2O_3 for which the tetravalent ground-state configuration is preferred. Incidentally, these are also the only sesquioxides that do not occur in nature. In the trivalent ground state, the sesquioxides are found to be insulators, with energy gaps of around 0.5 eV for the C form and around 2.7 eV for the A form. The corresponding DOS for the A-type Pu_2O_3 is shown in Fig. 3.

The ferromagnetic ordering was investigated for the cubic structure while the antiferromagnetic ordering of spins was studied for the hexagonal structures, and the values for the insulating gaps in Table II refer to these respective magnetic orderings. The bulk moduli for A-type Pu_2O_3, Am_2O_3, Cm_2O_3, Bk_2O_3, and Cf_2O_3 are similar in magnitude, calculated to be, respectively, 158, 158, 168, 166, and 174 GPa. No experimental measurements of the bulk moduli seem to exist but the value for Pu_2O_3 lies within the range of values obtained by Prodan *et al.*[39] and Jomard *et al.*[12] for a suite of different functionals (from 110 to 181 GPa). As can be seen from Table II, the calculated equilibrium volumes of the A-type sesquioxides are found to be in good agreement with experiment. This agreement is somewhat less satisfying for the C-type sesquioxides, where the volume is overestimated by up to 7%, which might be related to our approximate treatment of the actual bixbyite structure.

C. Actinide dioxides

1. Background information

The actinide dioxides from U to Cf have all been synthesized, crystallizing in the fluorite (CaF_2) structure. They are also the most relevant systems for applications and, as

TABLE III. Actinide dioxide data: Column 2: ground-state configuration. Columns 3 and 4: energy gaps, E_{gap}^{SIC} (this work) and E_{gap}^{HSE} (Ref. 47), respectively (in units of eV). Columns 5 and 6: calculated, a_0^{SIC}, and experimental a_0^{exp} lattice parameters (in Å). Column 7 and 8: calculated, B_0^{SIC}, and experimental, B_0^{exp}, bulk modulii (in units of GPa).

	Config.	E_{gap}^{SIC}	E_{gap}^{HSE}	a_0^{SIC}	a_0^{exp} [a]	B_0^{SIC}	B_0^{exp}
UO_2	f^1 (U^{5+})	0	2.4	5.40	5.470	219	207[b]
UO_2	f^2 (U^{4+})	2.6	2.4	5.47	5.470	219	207[b]
NpO_2	f^3 (Np^{4+})	2.3	3.1	5.46	5.433	217	200[b]
PuO_2	f^4 (Pu^{4+})	1.2	2.7	5.44	5.396	214	178[b]
AmO_2	f^5 (Am^{4+})	0.8	1.6	5.42	5.374	209	205[b]
CmO_2	f^6 (Cm^{4+})	0.4	0.4	5.37	5.359	212	218[c]
BkO_2	f^7 (Bk^{4+})	1.0	2.5	5.36	5.331	221	
CfO_2	f^8 (Cf^{4+})	0.6	2.0	5.36	5.310	210	

[a]Reference 33.
[b]Reference 67.
[c]Reference 68.

a consequence, are the most studied actinide oxide compounds, both experimentally and theoretically.[10,12,36,38,40,42–55] On the experimental side, a comprehensive summary of their electronic, magnetic, transport, and optical properties can be found in Troć *et al.*[52] The absence of features at the Fermi level in the observed XPS spectra[38] indicates that all the dioxides are semiconductors or insulators. However, specific information regarding the gap is only known for UO_2, NpO_2, and PuO_2. A combined XPS and bremsstrahlung isochromat spectroscopy spectrum for UO_2 finds an $O(2p) \rightarrow U(6d)$ gap of about 5 eV.[53] This value for the energy gap is similar to the one observed for ThO_2 but with the difference that in UO_2 two occupied rather well-localized f states are situated in the gap, with a $5f^2 \rightarrow 5f^1 6sd$ transition energy of 2–3 eV.[53,56] As the nuclear charge increases from Th to Pu, the f states move to lower energies. In ThO_2 the empty f states are situated in the Th sd derived conduction band. In UO_2 and NpO_2 the f states are occupied and situated in the energy band gap whereas in PuO_2 they are situated at the top of the O p derived valence band.[36] The measured activation energies, E_a=0.2 eV in UO_2, E_a=0.4 eV in NpO_2, and E_a=1.8 eV in PuO_2 confirm this trend.[54]

Electronic-structure calculations, in particular, for UO_2 and PuO_2, have shown that the itinerant f-electron picture is not adquate for describing these compounds. It has emerged that the LSD approximation wrongly predicts metallic behavior,[10,12,42] demonstrating the need to go beyond the homogeneous electron gas in describing the strong on-site f-electron correlations. So far, a number of calculations have shown that an insulating solution can be obtained when using improved descriptions of electron correlations such as those contained in the LDA(GGA)+U,[12,40,43,44,48] DMFT,[45] SIC-LSD,[46] and hybrid functional methodologies.[47]

2. SIC-LSD electronic structure

In the present paper the electronic structures of the dioxides from UO_2 to CfO_2 have been calculated using the SIC-LSD method. As can be seen from Table III, a tetravalent ground-state configuration is found for all the dioxides, except UO_2 where the pentavalent [$U(f^1)$] configuration is energetically more favorable. Actually, the pentavalent $U(f^1)$ and tetravalent $U(f^2)$ configurations are energetically close, with the f^1 configuration being more favorable by $\simeq$100 meV. Our calculations refer to T=0 K whereas the experimental evidence, which clearly indicates a tetravalent (insulating) UO_2, mostly refers to room-temperature conditions. Experiments also indicate a lattice expansion with temperature[57,58] but the f^1 to f^2 localization transition that our calculations seem to predict has not been observed experimentally. The prediction of an U f^1 ground-state configuration could possibly be related to the tetrad effect (multiplet formation energy),[59–61] which is ignored in our calculation, and which favors the f^2 configuration over the f^1 configuration. In the following, when comparing to experiment, we will be referring to the tetravalent UO_2 configuration as the ground-state configuration.

All the dioxides (including the tetravalent UO_2) are predicted to be insulators. The AFII magnetic ordering (i.e., ferromagnetically ordered planes stacked antiferrormagnetically along the [111] crystal direction) has been assumed in the dioxide calculations to which the SIC-LSD data in Table III refer. With respect to the band gap of UO_2, a value of E_{gap}=2.6 eV is found, which is smaller than the experimentally observed $p \rightarrow d$ gap, and which should not be compared to the optical gap referred to in the GGA+U (1.8 eV) and HSE (2.4 eV) calculations. The SIC-LSD approach, being an orbital-dependent DFT method, does not give accurate removal energies of localized states. The reason is that, unlike for the itinerant electron states within LDA, the exchange-correlation energy functional is not a good representation of the self-energy for those localized electron states. Therefore, to make contact with spectroscopy, one would have to consider the missing screening/relaxation effects, e.g., through the so-called Δ_{SCF} (Refs. 62 and 63) calculations, a Slater transition state,[64,65] or most desirably by combining the SIC with the GW approach.[66] Since in this work we concentrate on the total-energy differences and not on spectroscopy, the latter effects have not been accounted for. As a result, the

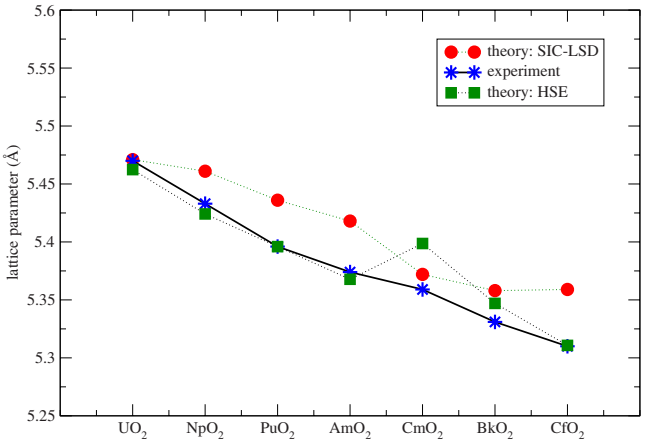

FIG. 4. (Color online) Lattice parameters of the actinide dioxides. Experimental values (Ref. 33) (blue stars) are compared to the theoretical SIC-LSD values (red circles), and the theoretical HSE values (green squares) read from the corresponding Fig. 1 in Ref. 47.

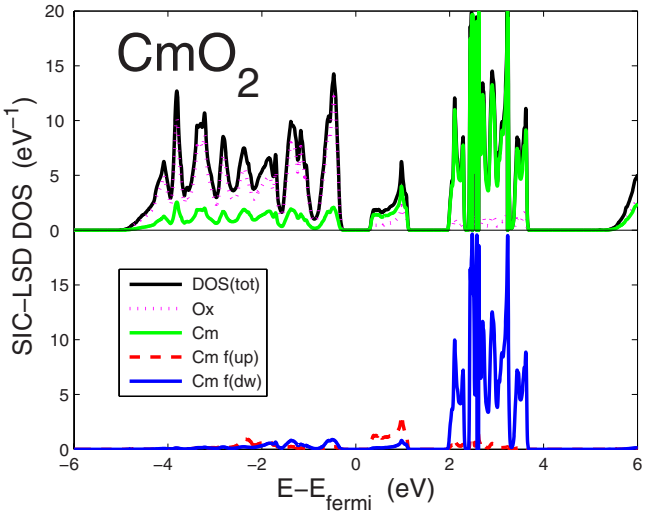

FIG. 5. (Color online) DOS of CmO_2. Upper panel: Total (black), Cm (green), and O (red dotted) DOSs. Lower panel: the corresponding Cm f majority (red) and minority (blue) spin decomposed DOSs. The energy is in eV relative to the Fermi level, which is situated midgap. Only the itinerant f states are shown.

present SIC-LSD calulations do not reproduce the correct position of the occupied f peak which is expected to be situated in the gap for both UO_2 or NpO_2. The Mott-insulating character ($f \rightarrow f$ transition) of the early dioxides[43,47] is thus not reproduced in our calculations, which instead describe the entire series as charge-transfer insulators ($p \rightarrow f$ transition). From PuO_2 onward, the occupied f states start moving into the valence band, and the charge-transfer picture becomes adequate for describing the nature of the gap. There exist only a few calculations dealing with the electronic structure of the heavy actinide dioxides.[35,47,49] In the following we make a detailed comparison with the recent results obtained by Prodan *et al.*[47] using the hybrid functional theory.

Both the SIC-LSD and the hybrid functional calculations determine the antiferromagnetic ground-state configuration as energetically most favorable. As can be seen in Table III, our calculated energy gaps are smaller than the corresponding HSE gaps but the trends agree, i.e., the gaps decrease from PuO_2 to CmO_2, and then again from BkO_2 onward. This reflects the gradual progression toward lower energy of the unoccupied f states, with increasing atomic number. The calculated lattice parameters are in very good agreement with experiment, within 1%, as seen in both Table III and Fig. 4. We should note here that the experimentally observed lattice parameters refer to room-temperature measurements,[33] and are thus on average larger than the values one would expect for $T=0$ K by approximately 0.011 Å.[69] The consistent overestimation of the lattice parameters is quite common for SIC-LSD, which has tendency to slightly overlocalize.

The overall experimental situation with regard to CmO_2 is still not fully understood.[70] It has been shown that, for a range of off-stoichiometric compounds CmO_{2-x}, both the lattice parameter and magnetic moment increase with x.[71–73] Given the expected moments of Cm^{3+} ($5f^7$; $\mu_{eff}=7.94\mu_B$) and Cm^{4+} ($5f^6$; $\mu_{eff}=0\mu_B$) it was noted that this trend indicates an increase in the number of Cm^{3+} impurities as we move away from stoichiometry. Based on the ionic picture, one accordingly expects the Cm^{4+} ground-state configuration for the stoichiometric compound, which however seems to be contradicted by the fact that in samples very close to stoichiometry[74] susceptibility measurements give the effective moment as high as $\mu_{eff}=3.36\mu_B$. Attempts to explain this discrepancy range from a possible existence of an impurity phase, not registered in the experiments, to assuming a covalent, rather than an ionic, picture for the ground state.[70] It has also been conjectured that a more complex ground state which includes some admixture of the excited $J=1$ state of Cm^{4+} might be required.[74]

The lattice-parameter measurements yield two different values for CmO_2, depending on whether the short-lived curium isotope of mass number 244 is used ($a=5.372$ Å) (Ref. 75) or the long-lived curium isotope of mass number 248 is used ($a=5.359$ Å).[72] The reason for this discrepancy has been traced to the self-radiation induced expansion that occurs with the considerably more active ^{244}Cm isotope.[72,73] It is the $^{248}CmO_2$ lattice parameter, i.e., without the effect of self-heating, that should be of relevance when comparing to the calculated lattice parameters.

From the SIC-LSD calculations we find the ground state of CmO_2 to be tetravalent and the corresponding lattice parameter is in good agreement with experiment. In Fig. 5 we show the DOS of CmO_2 in the Cm^{4+} (f^6) ground-state configuration. Here, similar to the DOS in Figs. 2 and 3, the localized f states are not shown, as they occur at too high binding energies. The compound is found to be insulating, with the Fermi level positioned between the completely filled O p band and the one remaining delocalized empty majority f-spin state that strongly hybridizes with the O p states. The resulting electronic structure is thus quite different from the hybrid functional picture, where the HSE applied by Prodan *et al.* results in metallic CmO_2. The authors suggest a covalent picture with significant Cm^{3+} character, as a result of the Cm trying to achieve the stable half-filled f-shell configura-

tion. Consequently some of the O p states are charge transferred to the Cm ion, resulting in the Fermi-level cutting across the top of the hybridized O p-Cm f band. However, unlike for all the other actinide dioxides, the lattice parameter of CmO_2, calculated using the HSE functional, deviates considerably from the measured value, as can be seen from Fig. 4.

With respect to the SIC-LSD calculations, one could envisage that a Cm^{3+} configuration in CmO_2 could be energetically favorable, given the associated half-filled f shell. Due to one less f state taking part in bonding, as compared to the Cm^{4+} ion, this in return could explain the slight increase in the experimentally observed lattice parameter of CmO_2. As it turns out, however, the total energy of the trivalent configuration is higher by 0.68 eV, indicating that the Cm^{4+} configuration is energetically very stable. The reason for this stability is related to the fact that localizing an additional electron in CmO_2 results in the Fermi level moving down into the p band. This implies a depopulation of the p band, as charge is transferred to the low lying f levels, and the associated loss in, respectively, the Madelung and hybridization energies is significantly larger than the gain in the f-localization energy. This charge-transfer picture is similar to the picture found in the hybrid functional theory. However, in variance to the conclusion of that work, we find the corresponding trivalent configuration to be energetically unfavorable.

Although our calculated ground state of CmO_2 finds a localized f^6 Cm ion, the system turns out to be magnetic. The ideal f^6 ion has $J=0$ and hence also $\langle S_z\rangle=0$ and $\langle L_z\rangle=0$ but this state is a linear combination of several six-electron Slater determinants, which we cannot realize in our SIC-LSD scheme. Rather, it may be represented by a single Slater determinant having $\langle S_z\rangle=3$ and $\langle L_z\rangle=-3$ (simulating antiparallel $S=3$ and $L=3$), which constitutes the starting point for our calculations before iteration to self-consistency. Spin-orbit coupling and hybridization significantly distort this initial configuration, in fact almost quenching the orbital moment. The total spin and orbital moment projections along the z axis are calculated to be $\langle S_z\rangle=2.73$ and $\langle L_z\rangle=-0.25$ (in units of $\hbar$). This comes from contributions from the localized f^6 ion ($\langle S_z\rangle=2.76$ and $\langle L_z\rangle=-1.15$) and from the delocalized f-band states ($\langle S_z\rangle=-0.03$ and $\langle L_z\rangle=+0.93$). The latter are largely tails of the O p-band states, which inside the atomic sphere around Cm attain f character. The total number of delocalized f-character states is 0.86, leading to a total f count of 6.86, which reflects a significant f hybridization with the O p bands. Assuming now, that the magnetic moment is given as $\mu=\langle 2S_z+L_z\rangle\mu_B$, we arrive at a total moment of $\mu=5.21\mu_B$ per Cm atom, which exceeds the experimental moment of $\mu_{eff}=3.36\mu_B$,[74] however demonstrating that the insulating state of CmO_2 may be magnetic. The quoted experimental moment is extracted from the large temperature magnetic susceptibility while the present theory is valid only at $T=0$. Furthermore, as stated, the fact that quantum fluctuations (more than one Slater determinant representing the localized f^6 shell), are not possible within the SIC-LSD approach, might be a serious limitation with respect to a proper description of magnetic properties. Thermal fluctuations can be considered using the so-called local SIC approach, implemented in the multiple-scattering theory, in combination with the coherent-potential approximation and disordered local-moment theory.[76,77]

Our calculations show that the nominal ionic $A^{4+}O_2^{2-}$ scenario is energetically favorable for all the dioxides, except for UO_2. The more delocalized nature of the f states in UO_2 would seem to indicate covalent bonding, as has been suggested by Moore *et al.*[78] based on their spin-orbit sum-rule analysis of electron-energy-loss spectroscopy measurements on actinide oxides. However this same study finds covalent bonding to also apply for PuO_2, at variance with our calculated tetravalent ground state, where four localized f electrons on each Pu ion indicate ionic bonding, in agreement with a recent DMFT study.[79]

3. Oxidation and reduction energies

In this section we will investigate the oxidation/reduction in the actinide dioxides, based on the SIC-LSD total energies involved in the different delocalization/localization transitions of the f electrons studied in this work. Specifically, we will be mostly concerned with the influence of the degree of f-electron localization on oxidation/reduction processes. The insertion/removal of O, apart from involving complex oxidation chemistry,[80] is bound to lead to considerable changes in the structure of the dioxide, and the resulting relaxations will no doubt influence the oxidation/reduction processes. However the hope is that these structural features will affect the whole dioxide series in a similar manner, regardless of which specific actinide ion is involved. We believe that the relaxations alone cannot explain the observed, rather dramatic, changes in oxidation patterns of the naturally occurring oxides, and, in particular, why the early actinides oxidize far more readily than the late actinides. These trends seem more likely to be governed by the character of the f electrons in a specific compound and its gradual change and the chemistry across the entire series. To study this link between oxidation/reduction and f electrons, we will assume the idealized crystal structures, with no atom relaxations, dictated by the fact that we use the ASA-based method.

Whether the oxidation or reduction process actually takes place depends on the thermodynamic conditions such as temperature, pressure, and, in particular, the O chemical potential. Since, however, the calculations have been performed at $T=0$ K, no entropic contribution to the free energy can be accounted for and therefore we express the reduction energy as

$$E^{red}=\frac{1}{4}[E(A_4O_6)+E(O_2)-E(A_4O_8)]. \tag{6}$$

Here $E(O_2)$ is the total energy of the oxygen molecule while $E(A_4O_8)$ and $E(A_4O_6)$ represent the total energies of, respectively, the dioxide and sesquioxide in the ground-state configuration as determined from the SIC-LSD calculations.

To study the oxidation reaction we construct the superstoichiometric oxide A_4O_9 by introducing one additional O into a four formula units AO_2 supercell. The CaF_2 structure is assumed to remain undistorted, with the extra O placed at the interstitial octahedral site of the resulting A_4O_9 compound. Applying the SIC-LSD to this hypothetical com-

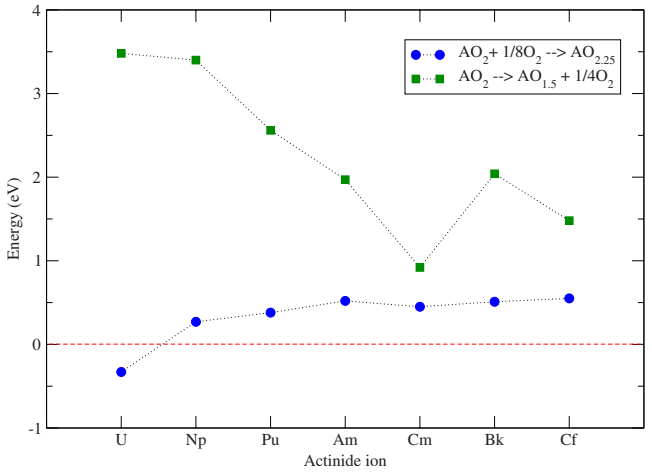

FIG. 6. (Color online) Estimated oxidation (circles) and reduction (squares) energies of the actinide dioxides according to the definitions in Eqs. (7) and (6). Energies are in eV per AO_2 unit cell.

pound, we find that the ground-state configuration changes gradually from the pentavalent U ions in $U_4^{5+}O_9$, to the tetravalent Cf ions in $Cf_4^{4+}O_9$. Compared to the tetravalent dioxide, A_4O_8, we observe that the inclusion of O impurities leads to f-electron delocalization in the early actinide oxides U_4O_9, Np_4O_9, and Pu_4O_9, whereas from Am_4O_9 onward the compounds remain tetravalent. Having calculated the ground-state configuration and total energy of A_4O_9, we can define the corresponding oxidation energy as

$$E^{ox} = \frac{1}{4}\left[E(A_4O_9) - E(A_4O_8) - \frac{1}{2}E(O_2) \right]. \quad (7)$$

The calculated reducton and oxidation energies of Eqs. (6) and (7) are presented in Fig. 6, where the value of 7.2 eV has been adopted as a binding energy of the O_2 molecule (relative to the nonspin-polarized O atoms; the atomic spin-polarization energy[81] is 1.14 eV per O atom). It emerges from the figure that E^{ox} increases slightly and E^{red} decreases as we move through the actinide series, which reflects the increasing f-electron binding energy. In Uranium an f electron is readily promoted into the valence band to facilitate uptake of superstoichiometric oxygen while this becomes increasingly more difficult with heavier actinides. On the other hand the U f manifold is very reluctant to take on an extra f electron to form the 3+ ion on reduction while this becomes easier for the later actinides. The jump in reduction energy at Bk reflects the relative stability of the half-filled f^7 shell in BkO_2.

According to the calculated energy differences, the only compound that oxidizes exothermically is UO_2 while for all the other actinide dioxides the energy balance is positive and increasing with actinide atomic number. This result is in overall good agreement with experimental data. UO_{2+x} has been synthesized up to $x=0.25$ (U_4O_9). The crystal structure remains fluorite based, with the excess O atoms situated at interstitial sites.[82] With respect to Np compounds, the only known stable binary oxide, apart from NpO_2, is Np_2O_5 with a structure that can no longer be described as underlying fluorite.[83] In particular, the fluorite derived Np_4O_9 does not seem to exist. With regards to PuO_{2+x}, the present calculations confirm the stability of PuO_2, in line with the majority of experimental investigations on this material. The same conclusion was reached in an earlier SIC-LSD study[46] where the possible discovery of a higher composition binary oxide, PuO_{2+x} ($x \leq 0.27$) (Ref. 84) was discussed. Beyond Pu there have been no reports of superstoichiometric oxides. The positive, slightly increasing, oxidation energies in Fig. 6 confirm that the dioxide for all the transplutonium actinides is increasingly stable against oxidation.

Concerning the reduction reaction in Eq. (6), it is found that the energy balance always favors the dioxide. With respect to the early actinides U and Np, the large value of the reduction energy is in agreement with the experimental fact that neither U_2O_3 nor Np_2O_3 exists. The sesquioxides from Pu_2O_3 to Cf_2O_3 do exist, however, according to our calculations, they are, in principle, unstable in air toward further uptake of oxygen and formation of the dioxide. In practice, there may be appreciable barriers to the actual transformation,[85] which furthermore may be influenced by thermodynamic conditions (temperature and pressure) not considered here.

IV. SUMMARIZING DISCUSSION

From the study of the stable binary actinide oxides, a clear picture emerges that links the degree of oxidation to the degree of f-electron localization. In the early actinides, the f electrons are less bound to the actinide ions which translates into valencies as high as 5+ and 6+ for U oxides, for example. As one progresses through the actinide series, the f electrons become increasingly tightly bound to the actinide ion and eventually, for Cf only the 3+ valency occurs naturally. The actinide ions play an active role in accomodating extra O, as their localized f electrons can act as electron reservoirs for the highly electronegative O ion. In other words, whether the oxidation is favored depends on the willingness of the actinide to delocalize further f electrons. From the SIC-LSD study we find that the divalent configuration is never favored, except maybe for EsO. Consequently, the monoxide never forms as the third electron is readily delocalized and made available for oxidation, which leads to the formation of trivalent sesquioxides. Whether the oxidation progresses further to produce the corresponding dioxide depends on delocalization of the fourth electron on the actinide ion. As we have seen, this delocalization is less likely to happen for the late actinides, where the f electrons tend to be more localized and where experiment shows that the synthesis of CfO_2 takes place under powerful oxidation conditions, e.g., in the presence of high-pressure molecular or atomic oxygen.[85] For the early actinides, on the other hand, the oxidation to the dioxide occurs readily and, for example, U_2O_3 and Np_2O_3 do not exist naturally. Finally, the further oxidation from dioxide to higher oxide only occurs for UO_2, where both the $5+(U_2O_5)$ and $6+(UO_3)$ U valencies exist, and for NpO_2 where the 5+ valency is obtained in Np_2O_5. We can speculate here as to whether the fact that we actually determine a marginally pentavalent ground state for UO_2

TABLE IV. Ground-state valency configurations of the actinide and lanthanide oxides. Bold lettering indicates that the corresponding compound actually exists in nature.

A	U	Np	Pu	Am	Cm	Bk	Cf	Es
AO	5+	4+	3+	3+	3+	3+	3+	**3+/2+**
A_2O_3	4+	4+	**3+**	**3+**	**3+**	**3+**	**3+**	
AO_2	**5+/4+**	**4+**	**4+**	**4+**	**4+**	**4+**	**4+**	
R	Nd	Pm	Sm	Eu	Gd	Tb	Dy	Ho
RO	3+	3+	**3+/2+**	**2+**	3+	3+	3+	3+
R_2O_3	**3+**	**3+**	**3+**	**3+**	**3+**	**3+**	**3+**	**3+**
RO_2	4+	4+	3+	3+	3+	**4+**	3+	3+

(rather than the well-established tetravalent configuration) is an indication that an additional *f* electron is on the brink of delocalization, thus favoring the formation of higher U oxides. The remaining dioxides are stable with respect to oxidation, as the gain in delocalizing the fifth electron is no longer favorable compared to the corresponding loss in SIC energy.

In Table IV we have collected our results of the SIC-LSD total-energy calculations for the actinide oxides (the upper four rows). The numbers indicate the ground-state valency configurations that we have determined for a given compound. Bold large letters are used to indicate those compounds that actually do exist in nature. It clearly emerges that only in those cases where the calculated ground-state valency agrees with the nominal charge expected from an ideal ionic picture, does the corresponding oxide seem to form. In other words, those oxides where our calculations predict a valency configuration that is not in agreement with simple charge counting will not form naturally, and the excess/shortage of charge indicates that oxidized/reduced compound will be favored instead. These trends emphasize the very ionic nature of bonding in the actinide oxides.

It is interesting to compare these trends in oxidation of the actinides to the corresponding behavior of the lanthanides.[86,87] In the latter the $4f$ electrons are overall more tightly bound to the lanthanide ion, which will favor lower oxidation numbers, compared to the spatially more extended $5f$ electrons. The corresponding calculated valency configurations[86] are shown in Table IV (the lower four rows). The effect of the increased localization can be observed from the fact that a number of the lanthanide monoxides actually exists, and it emerges from SIC-LSD studies that especially for the half-filled and filled shell *f*-electron systems, i.e., for EuO and YbO, the divalent configuration is energetically most favorable. All the lanthanide sesquioxides occur in nature, and the ground-state configuration of the corresponding lanthanide ions is trivalent. Even though the $4f$ electrons tend to be more localized, the 3+ valency occurs naturally, which is in agreement with the trivalent configuration being the most favorable for the lanthanide metals. With respect to further oxidation to the tetravalent dioxide, only CeO_2, PrO_2, (not shown in Table IV), and TbO_2, are found to occur naturally or (for TbO_2) under high O pressure, indicating that an additional *f* electron only delocalizes in the very early lanthanides, i.e., in Ce and Pr, where the *f* electrons are less tightly bound or in the middle of the series, where tetravalent TbO_2 is favored by the half-filled shell configuration.[86] Higher oxidation numbers than IV do not exist for the lanthanide oxides. Again we observe that for those compounds that exist in nature the calculated ground-state valency agrees fully with the simple charge counting.

V. CONCLUSION

We have studied the electronic structure of actinide oxides, specifically monoxides, sesquioxides, and dioxides, within the *ab initio* SIC-LSD band-structure method. By studying the oxidation and reduction reactions we have been able to conclude that the dioxides, from Np onward, are the most stable compounds among the studied actinide oxides. Our study reveals a strong link between the preferred oxidation number and the degree of localization which is confirmed by comparing to the ground-state configurations of the corresponding lanthanide oxides. The ionic nature of the actinide oxides is reflected in that for those compounds that exist in nature, the calculated ground-state valency agrees with the nominal valency expected from a simple charge counting.

ACKNOWLEDGMENTS

This research used resources of the Danish Center for Scientific Computing (DCSC) and of the National Energy Research Scientific Computing Center (NERSC). Work of one of us (G. M. S.) is supported by US Department of Energy, Office of Basic Energy Sciences, as part of an Energy Frontier Research Center. We gratefully acknowledge helpful discussions with M. S. S. Brooks.

*leon.petit@stfc.ac.uk

[1] G. R. Choppin, J. O. Liljenzin, and J. Rydberg, *Radiochemistry and Nuclear Chemistry*, 3rd ed. (Butterworth-Heinemann, Woburn, MA, 2001), Chap. 21.

[2] R. J. M. Konings, J. Nucl. Mater. **298**, 255 (2001).

[3] M. Beauvy, T. Duverneix, C. Berlanga, R. Mazoyer, and C. Duriez, J. Alloys Compd. **271-273**, 557 (1998).

[4] F. Weigel, J. J. Katz, and G. T. Seaborg, in *The Chemistry of the Actinide Elements*, edited by J. J. Katz, G. T. Seaborg, and L. R. Morss (Chapman Hall, New York, 1986), Vol. 1, p. 680.

[5] C. Guéneau, C. Chatillon, and B. Sundman, J. Nucl. Mater. **378**, 257 (2008).

[6] B. Johansson and H. Skriver, J. Magn. Magn. Mater. **29**, 217 (1982).

[7] A. Svane, L. Petit, Z. Szotek, and W. M. Temmerman, Phys. Rev. B **76**, 115116 (2007).
[8] K. T. Moore and G. van der Laan, Rev. Mod. Phys. **81**, 235 (2009).
[9] T. Maehira and T. Hotta, J. Magn. Magn. Mater. **310**, 754 (2007).
[10] J. C. Boettger and A. K. Ray, Int. J. Quantum Chem. **90**, 1470 (2002).
[11] M. Freyss, N. Vergnet, and T. Petit, J. Nucl. Mater. **352**, 144 (2006).
[12] G. Jomard, B. Amadon, F. Bottin, and M. Torrent, Phys. Rev. B **78**, 075125 (2008).
[13] V. I. Anisimov, J. Zaanen, and O. K. Andersen, Phys. Rev. B **44**, 943 (1991).
[14] A. B. Shick, A. I. Liechtenstein, and W. E. Pickett, Phys. Rev. B **60**, 10763 (1999).
[15] G. Kotliar and D. Vollhardt, Phys. Today **57**(3), 53 (2004).
[16] S. Y. Savrasov, G. Kotliar, and E. Abrahams, Nature (London) **410**, 793 (2001).
[17] A. D. Becke, J. Chem. Phys. **98**, 1372 (1993).
[18] J. P. Perdew and A. Zunger, Phys. Rev. B **23**, 5048 (1981).
[19] D. Kasinathan, J. Kuneš, K. Koepernik, C. V. Diaconu, R. L. Martin, I. D. Prodan, G. E. Scuseria, N. Spaldin, L. Petit, T. C. Schulthess, and W. E. Pickett, Phys. Rev. B **74**, 195110 (2006).
[20] W. M. Temmerman, A. Svane, Z. Szotek, H. Winter, and S. V. Beiden, in *Lecture Notes in Physics*, edited by M. Dreyssé (Springer-Verlag, Berlin, 2000), Vol. 535, p. 286.
[21] A. Svane, Phys. Rev. B **53**, 4275 (1996).
[22] O. K. Andersen, Phys. Rev. B **12**, 3060 (1975).
[23] P. Larson, W. R. L. Lambrecht, A. Chantis, and M. van Schilfgaarde, Phys. Rev. B **75**, 045114 (2007).
[24] G. C. Allen and P. M. Tucker, J. Chem. Soc. Dalton Trans. 1973, 470.
[25] W. P. Ellis, Surf. Sci. **61**, 37 (1976).
[26] D. J. Lam, J. B. Darby, and M. B. Newitt, in *The Actinides, Electronic Structure and Related Properties*, edited by A. J. Freeman and J. B. Darby (Academic, New York, 1974), Vol. 11, p. 119.
[27] K. Winer, C. A. Colmenares, R. L. Smith, and F. Wooten, Surf. Sci. **177**, 484 (1986).
[28] M. Eckle and T. Gouder, J. Alloys Compd. **374**, 261 (2004).
[29] K. Richter and C. Sari, J. Nucl. Mater. **148**, 266 (1987).
[30] J. R. Naegele, L. E. Cox, and J. W. Ward, Inorg. Chim. Acta **139**, 327 (1987).
[31] Y. Akimoto, J. Inorg. Nucl. Chem. **29**, 2650 (1967).
[32] J. Fahey, J. Peterson, and R. Baybarz, Inorg. Nucl. Chem. Lett. **8**, 101 (1972).
[33] P. Villars and L. D. Calvert, *Pearson's Handbook of Cystallographic Data for Intermetallic Phases*, 2nd ed. (ASM International, Ohio, 1991).
[34] M. S. S. Brooks, J. Phys. F: Met. Phys. **14**, 639 (1984).
[35] V. A. Gubanov, A. Rosén, and D. E. Ellis, J. Phys. Chem. Solids **40**, 17 (1979).
[36] D. Courteix, J. Chayrouse, L. Heintz, and R. Baptist, Solid State Commun. **39**, 209 (1981).
[37] T. Gouder, P. M. Oppeneer, F. Huber, F. Wastin, and J. Rebizant, Phys. Rev. B **72**, 115122 (2005).
[38] B. W. Veal, D. J. Lam, and H. R. Hoekstra, Phys. Rev. B **15**, 2929 (1977).
[39] I. D. Prodan, G. E. Scuseria, and R. L. Martin, Phys. Rev. B **73**, 045104 (2006).
[40] B. Sun, P. Zhang, and X. G. Zhao, J. Chem. Phys. **128**, 084705 (2008).
[41] M. Wulff and G. H. Lander, J. Chem. Phys. **89**, 3295 (1988).
[42] J. C. Boettger and A. K. Ray, Int. J. Quantum Chem. **80**, 824 (2000).
[43] Y. Yun, H. Kim, H. Kim, and K. Park, Nuclear Engineering and Technology **37**, 293 (2005).
[44] S. L. Dudarev, G. A. Botton, S. Y. Savrasov, Z. Szotek, W. M. Temmerman, and A. P. Sutton, Phys. Status Solidi A **166**, 429 (1998).
[45] Q. Yin and S. Y. Savrasov, Phys. Rev. Lett. **100**, 225504 (2008).
[46] L. Petit, A. Svane, Z. Szotek, and W. M. Temmerman, Science **301**, 498 (2003).
[47] I. D. Prodan, G. E. Scuseria, and R. L. Martin, Phys. Rev. B **76**, 033101 (2007).
[48] B. Dorado, B. Amadon, M. Freyss, and M. Bertolus, Phys. Rev. B **79**, 235125 (2009).
[49] P. J. Kelly, M. S. S. Brooks, and R. Allen, J. Phys. (Paris) **40**, C4-184 (1979).
[50] P. J. Kelly and M. S. S. Brooks, J. Chem. Soc., Faraday Trans. 2 **83**, 1189 (1987).
[51] B. Johansson, J. Phys. Chem. Solids **39**, 467 (1978).
[52] R. Troć and D. Kaczorowski, in *Group III Condensed Matter*, Landolt-Bornstein, New Series, Group III, Vol. 27, Pt. C2, edited by H. J. Wijn (Springer, Berlin, 1999).
[53] Y. Baer and J. Schoenes, Solid State Commun. **33**, 885 (1980).
[54] J. M. Fournier and R. Troć, in *Handbook on the Physics and Chemistry of the Actinides*, edited by A. J. Freeman and G. H. Lander (North Holland, Amsterdam, 1985), Vol. 2, Chap. 2.
[55] P. Santini, S. Carretta, G. Amoretti, R. Caciuffo, N. Magnani, and G. H. Lander, Rev. Mod. Phys. **81**, 807 (2009).
[56] J. Schoenes, J. Chem. Soc., Faraday Trans. 2 **83**, 1205 (1987).
[57] O. G. Brandt and C. T. Walker, Phys. Rev. Lett. **18**, 11 (1967).
[58] K. H. Kang, H. J. Ryu, K. C. Song, and M. S. Yang, J. Nucl. Mater. **301**, 242 (2002).
[59] C. Jorgensen, *Orbitals in Atoms and Molecules* (Academic, London, 1962).
[60] L. J. Nugent, J. Inorg. Nucl. Chem. **32**, 3485 (1970).
[61] S. Xia and J. C. Krupa, J. Alloys Compd. **307**, 61 (2000).
[62] A. J. Freeman, B. Min, and M. R. Norman, *Handbook on the Physics and Chemistry of Rare Earths*, edited by K. A. Gschneidner, Jr., L. Eyring, and S. Hüfner (Elsevier, Amsterdam, 1987), Vol. 10.
[63] W. M. Temmerman, Z. Szotek, and H. Winter, Phys. Rev. B **47**, 1184 (1993).
[64] J. C. Slater, Adv. Quantum Chem. **6**, 1 (1972).
[65] J. G. Harrison, R. A. Heaton, and C. C. Lin, J. Phys. B **16**, 2079 (1983).
[66] F. Aryasetiawan and O. Gunnarsson, Rep. Prog. Phys. **61**, 237 (1998).
[67] M. Idiri, T. Le Bihan, S. Heathman, and J. Rebizant, Phys. Rev. B **70**, 014113 (2004).
[68] J. P. Dancausse, R. G. Haire, S. Heathman, and U. Benedict, J. Nucl. Sci. Technol **3**, 136 (2002).
[69] U. Benedict and C. Dufour, Physica B & C **102**, 303 (1980).
[70] L. Soderholm, J. Less-Common Met. **133**, 77 (1987).
[71] S. E. Nave, R. G. Haire, and P. G. Huray, Phys. Rev. B **28**, 2317 (1983).
[72] J. R. Peterson and J. Fuger, J. Inorg. Nucl. Chem. **33**, 4111

(1971).
[73] M. Noé and J. Fuger, Inorg. Nucl. Chem. Lett. **7**, 421 (1971).
[74] L. R. Morss, J. W. Richardson, C. W. Williams, G. H. Lander, A. C. Lawson, N. M. Edelstein, and G. V. Shalimoff, J. Less-Common Met. **156**, 273 (1989).
[75] L. B. Asprey, F. H. Ellinger, S. Fried, and W. H. Zachariasen, J. Am. Chem. Soc. **77**, 1707 (1955).
[76] M. Lüders, A. Ernst, M. Däne, Z. Szotek, A. Svane, D. Ködderitzsch, W. Hergert, B. L. Gyorffy, and W. M. Temmerman, Phys. Rev. B **71**, 205109 (2005).
[77] I. D. Hughes, M. Däne, A. Ernst, W. Hergert, M. Lüders, J. P. Poulter, J. B. Staunton, A. Svane, Z. Szotek, and W. M. Temmerman, Nature (London) **446**, 650 (2007).
[78] K. T. Moore, G. van der Laan, R. G. Haire, M. A. Wall, and A. J. Schwartz, Phys. Rev. B **73**, 033109 (2006).
[79] J. H. Shim, K. Haule, and G. Kotliar, EPL **85**, 17007 (2009).
[80] D. A. Andersson, J. Lezama, B. P. Uberuaga, C. Deo, and S. D. Conradson, Phys. Rev. B **79**, 024110 (2009).
[81] E. L. Peltzer y Blancá, A. Svane, N. E. Christensen, C. O. Rodriguez, O. M. Cappannini, and M. S. Moreno, Phys. Rev. B **48**, 15712 (1993).
[82] G. C. Allen, P. M. Tucker, and J. W. Tyler, J. Phys. Chem. **86**, 224 (1982).
[83] T. Forbes, P. Burns, S. Skanthakumar, and L. Soderholm, J. Am. Chem. Soc. **129**, 2760 (2007).
[84] J. M. Haschke, T. H. Allen, and L. A. Morales, Science **287**, 285 (2000).
[85] R. D. Baybarz, R. G. Haire, and J. A. Fahey, J. Inorg. Nucl. Chem. **34**, 557 (1972).
[86] L. Petit, A. Svane, Z. Szotek, and W. M. Temmerman, Phys. Rev. B **72**, 205118 (2005).
[87] L. Petit, A. Svane, Z. Szotek, and W. M. Temmerman, in *Topics in Applied Physics*, edited by M. Fanciulli and G. Scarel (Springer-Verlag, Berlin, 2007), Vol. 106, p. 331.